Derivatives of dipyrido[3,2-*a*:2′,3′-*c*]phenazine and its ruthenium complexes, influence of arylic substitution on photophysical properties†

Bernhard Schäfer,[a] Helmar Görls,[a] Martin Presselt,[b] Michael Schmitt,[b] Jürgen Popp,[b] William Henry,[c] Johannes G. Vos[c] and Sven Rau*[a]

Received 8th September 2005, Accepted 18th January 2006
First published as an Advance Article on the web 14th February 2006
DOI: 10.1039/b512773d

The synthesis and photophysical properties of a series of substituted dipyridophenazine (dppz) ruthenium complexes of the type $[(tbbpy)_2Ru(dppz\text{-}R_2)]^{2+}$ (where tbbpy = 4,4-*tert*-butyl-2,2-bipyridine and dppz = dipyrido[3,2-*a*:2′,3′-*c*]phenazine and R represents substitution at the 11 and 12 position with: Br, phenyl, 4-*tert*-butyl-phenyl and *para*-biphenyl) are described. The ligands could be obtained in high yields using Suzuki-type coupling reactions, an approach which also has been successfully applied to the analogous dppz-Br_2 ruthenium complex. All compounds are fully characterised by NMR, MS and UV-vis spectroscopy. The solid state structures of dppz-bi-*para*-biphenyl and the ruthenium complex $[(tbbpy)_2Ru(dppz\text{-}Br_2)]^{2+}$ are also reported. The investigation of the free ligands reveals a pronounced effect of the arylic substitution on absorption and emission properties. These properties are mirrored in the corresponding complexes, which possess emission lifetimes of up to 900 ns. The resonance Raman investigation of the complex $[(tbbpy)_2Ru(dppz\text{-}Br_2)]^{2+}$ supports the assumption that the excited state properties of the substituted complexes are related to the parent $[(bpy)_2Ru(dppz)]^{2+}$ compound, but that important differences may be expected based on the differences observed in the lowest energy absorption band.

Introduction

Ruthenium complexes with dipyrido[3,2-*a*:2′,3′-*c*]-phenazine (dppz) are intensively investigated due to their potential as luminescent DNA sensors[1–11] or as reversible electron carriers.[12] Both functions strongly depend on the role of the phenazine part of the dppz ligand as electron acceptor. In addition to this electronic role structural features of the ligand are equally important. For instance the planar geometry of the dppz ligand allows efficient intercalation with helical DNA which is observed with high equilibrium binding constants for Ru–DNA of up to 10^6 M^{-1}.[5] In view of these potential applications substantial efforts have been directed towards the design of new dppz-type ligand structures.[13–16]

To rationally design such new ligands it is helpful to consider the course of events following photoexcitation with visible light. For ruthenium dppz complexes an electron, formally originating from a d orbital on the ruthenium centre, is transferred to a π* orbital of the dppz ligand and this results in the formation of a long lived ^{3}MLCT state.[10,17–20] A currently discussed detailed mechanism for the population of this ^{3}MLCT involves initial population of the ^{1}MLCT localised on the bipyridine part of the dppz ligand with subsequent intraligand electron transfer to the phenazine based pyrazine moiety where the ^{3}MLCT is finally localised. It is generally accepted that it is this state that is responsible for the unique photophysical properties of these complexes.[21–23] The aim of this contribution is the preparation of novel ligands that will lead to metal complexes with significantly improved excited state properties, such as longer excited state lifetimes. This may be achieved by delocalisation of the charge in the final triplet state. One way of achieving this is by the introduction of phenyl-type substituents.

In this contribution we present a series of substituted dppz ligands and their corresponding ruthenium polypyridyl complexes, see Fig. 1. The reasons for their selection is outlined above but we also wish to emphasise that the development of an efficient synthetic method for introducing substituents in the dppz frame using organometallic reactions is also a major point in this study.

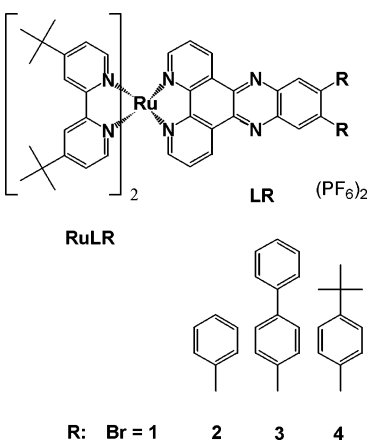

Fig. 1 Naming of ruthenium complexes and corresponding ligands.

[a]*Institut für Anorganische und Analytische Chemie, Friedrich-Schiller-Universität, Lessingstr. 8, 07743, Jena, Germany. E-mail: sven.rau@uni-jena.de; Fax: +49 3641 948102; Tel: +49 3641 948113*
[b]*Institut für Physikalische Chemie, Helmholzweg 4, Friedrich-Schiller-Universität, 07743, Jena, Germany*
[c]*National Centre for Sensor Research, School of Chemical Sciences, Dublin City University, Dublin 9, Ireland*

† Electronic supplementary information (ESI) available: Detailed NMR spectra of the ligands **LR** and complexes **RuLR**. See DOI: 10.1039/b512773d

To avoid solubility problems we utilised *tert*-butyl substituted complexes since this ensures high solubility in organic solvents. Since it has recently been emphasised that the substitution of the ancillary ligands may have an influence on the entantioselectivity of the interaction of the complexes with DNA,[24,25] we were also interested in obtaining more detailed structural information on substituted dppz–ruthenium complexes.

The novel ligands **L1** to **L4** have been prepared to illustrate the potential of the building block approach utilising organometallic C–C coupling reactions.

Experimental

Unless otherwise noted, all Pd catalyzed cross coupling reactions were conducted under an atmosphere of dry, deoxygenated argon using standard Schlenk techniques. $Ru(tbbpy)_2Cl_2$,[26] $phenO_2$[5] and 4,5-dibromo-*ortho*phenylendiamine[27] were prepared using literature methods. Acetonitrile was distilled from CaH_2. Toluene was distilled from sodium benzophenone ketyl under an argon atmosphere prior to use. All other solvents were used as received.

Infrared spectra were recorded using a Perkin-Elmer 2000 FT-IR; ^{1}H NMR spectra were recorded on a Bruker 400 MHz/200 Mhz spectrophotometer. The mass spectra were obtained using a SSQ 170, Finnigan MAT at the Friedrich Schiller University Jena. Electrospray-Mass spectra were recorded on a Finnigan MAT, MAT 95 XL. The positive ES mass spectra were obtained with voltages of 3–4 kV applied to the electrospray needle. The microwave assisted reactions were carried out using the Microwave Laboratory Systems MLS EM-2 microwave system.

Synthesis of Br_2dppz (L1)

Phendione (2 g, 9.5 mmol) and 4,5-dibromo-*ortho*phenylendiamine (2.534 g, 9.5 mmol) were refluxed in absolute EtOH (300 ml) for 8 h. The volume of the solvent was reduced to 50 ml and cooled in a refrigerator over night. $dppzBr_2$ was collected by filtration. Yield 90%. ^{1}H NMR (ppm; $CDCl_3$) 7.730 phen(2H, dd); 8.559 H4(2H, s); 9.233 phen(2H, d(lc)); 9.529 phen(2H, d(lc));EI-MS $m/z = 440$ (100%) matching isotopic pattern.

Typical procedure for preparation of L2 from uncoordinated Br_2dppz (L1)

A Schlenk vessel was charged with $dppzBr_2$ (0.250 g, 0.568 mmol) and the corresponding boronic acid (1.136 mmol), $Pd(PPh_3)_4$ (0.013 g, 0.0113 mmol (1.0 mol %)) in 50 ml dry toluene and 15 ml of oxygen free solution of 2 M aqueous Na_2CO_3. The suspension was refluxed under argon for three days. After cooling to room temperature the reaction mixture was taken up in 100 ml water followed by extraction with chloroform. The solvent of the combined organic layers was removed and the crude product dried under vacuum.

Column chromatography (using silica and a gradients eluent system starting with $CHCl_3$ and changing to $CHCl_3$/MeOH (9 : 1). The fluorescent main band was collected and yields pure **L2**. Yield 60–80%.

L2 ^{1}H NMR (ppm; $CDCl_3$) 7.305 phenyl (10H, s); 7.808 H2-phen (2H, dd); 8.363 H4 (2H, s); 9.300 H3-phen (2H, d); 9.626 H1-phen (2H, d); MS (DEI, EI+ Q1MS) $m/z = 434$ (100%) (M^+).

L3 ^{1}H NMR (ppm; d_6-DMSO) 7.43 H7, H8, H9 (10H, m); 7.70 H6, H5 (8H, m); 7.91 H2(2H, dd); 8.31 H4(2H, s); 9.19 H3(2H, d(lc)); 9.44 H1(2H, d(lc)). MS (DEI, EI+ Q1MS) $m/z = 586$ (100%) (M^+).

L4 ^{1}H NMR (ppm, CD_2Cl_2) 1.321 CH_3 (*tert*-butyl, 18H, s); 7.325 H6, H5(8H, m); 7.794 H3 (2H, dd); 8.361 H4 (2H, s); 9.215 H3 (2H, d(lc)); 9.622 H1 (2H, d(lc)); MS (DEI, EI+ Q1MS) $m/z =$ 546 (30%) (M^+), $m/z = 531$ (35%) ($M^+ - CH_3$).

Complexation of L1–L4

$Ru(tbbpy)_2Cl_2$ (0.1 g, 0.14 mmol) and the corresponding ligand (0.14 mmol) were suspended in DMF/H_2O (80 ml/10 ml) and heated at reflux for 3 h using microwave irradiation (150 W). The solvent was removed under reduced pressure. The complexes were recrystallized from an ethanol/aqueous NH_4PF_6 mixture and further purified using chromatography using a gradient changing from EtOH to EtOH/H_2O/KNO_3. Yield 80–85%. For a detailed assignment of the chemical shifts to the corresponding atom see the electronic supplementary information (ESI).†

RuL1 (ppm CD_3CN) 1.347 (18H, s); 1.441 (18H, s); 7.233 (2H, d); 7.466 (2H, d); 7.565 (2H, d); 7.659 (2H, d); 7.888 (2H, dd); 8.143 (2H,d); 8.476 (2H, s); 8.515 (2H, s); 8.844 (2H, s); 9.556 (2H, d) MS (ESI, MeOH,): $m/z = 1223.2$ ($[M - (PF_6)]^+$, 100%).

RuL2 (ppm CD_3CN) 1.327 (18H, s); 1.434 (18H, s); 7.256 (2H, d(lc)); 7.353 (10H, m); 7.475 (2H, d(lc)); 7.620 (2H, d); 7.694 (2H, d); 7.896 (2H, dd); 8.146 (2H, d(lc)); 8.422 (2H, s); 8.512 (2H, s); 8.551 (2H, s); 9.589 (2H, d) MS (ESI, MeOH,): $m/z = 1217.5$ ($[M - (PF_6)]^+$, 100%); $m/z = 536.4$ ($[M - 2(PF_6)]^{2+}$).

RuL3 (ppm CD_3CN) 1.277 (18H, s); 1.471 (18H, s); 7.412 (10H, m); 7.211 (4H, d); 7.272 (4H, d); 7.348 (2H, d); 7.522 (2H, d); 7.772 (4H, d); 7.799 (2H, dd); 7.968 (2H, s); 8.241 (2H, d); 8.571 (2H, s); 8.639 (2H, s); 9.175 (2H, d); MS (ESI, MeOH): $m/z = 1369.2$ ($[M - (PF_6)]^+$, 69%); $m/z = 611.9$ ($[M - 2(PF_6)]^{2+}$, 100%).

RuL4 (ppm CD_3CN) 1.312 (18H, s); 1.329 (18H, s); 1.468 (18H, s); 7.228 (8H, m); 7.328 (2H, d(lc)); 7.505 (2H, d(lc)); 7.703 (2H, d); 7.736 (2H, d); 7.774 (2H, dd); 8.031 (2H, s); 8.161 (2H, (lc)); 8.517 (2H, s); 8.566 (2H, s); 9.268 (2H, d(lc)) MS (ESI, MeOH): $m/z = 1329.0$ ($[M - PF_6]^+$, 100%), $m/z = 531$ ($[M - 2PF_6]^{2+}$, 20%).

Suzuki-reaction at the complex (RuL1)

$RuL1(PF_6)_2$ (0.150 g, 0.11 mmol), phenyl boronic acid (0.028 mg, 0.23 mmol) and $Pd(PPh_3)_4$ (12 mg, 8.8×10^{-6} mol (4 mol%)) were suspended in 50 ml acetonitrile and 15 ml of a oxygen free solution of 2 M aqueous Na_2CO_3 and refluxed for 3 days. After cooling to rt 100 ml of water were added followed by extraction with dichloromethane. The organic layers were collected, the solvent was removed under reduced pressure and the residue was cleaned by column chromatography collecting the main band (using silica, EtOH, EtOH/H_2O, KNO_3). Yield 67%. Analytical data obtained are identical to those observed for the sample obtained from complexation of **L2** to the ruthenium precursor.

Crystal structure determination

The intensity data for the compounds were collected on a Nonius Kappa CCD diffractometer, using graphite-monochromated

Mo-K_α radiation. Data were corrected for Lorentz and polarization effects, but not for absorption effects.[28,29]

The structures were solved by direct methods (SHELXS[30]) and refined by full-matrix least squares techniques against Fo^2 (SHELXL-97).[31] The hydrogen atoms (without the disordered toluene molecules of **L3**) were included at calculated positions with fixed thermal parameters. All non-hydrogen atoms were refined anisotropically.[31] XP (SIEMENS Analytical X-ray Instruments, Inc.) was used for structure representations. X-Ray suitable crystals of **RuL1** were grown from acetonitrile/hexane solutions.

Crystal data for RuL1. $C_{54}H_{56}Br_2F_{12}N_8P_2Ru{\cdot}2C_2H_3N$, M_r = 1450.01 g mol^{-1}, red-brown prism, size 0.03 × 0.03 × 0.02 mm^3, triclinic, space group $P\bar{1}$, a = 12.7435(3), b = 15.0747(3), c = 16.6350(4) Å, α = 91.617(1), β = 97.359(1), γ = 98.611(1)°, V = 3129.9(1) Å^3, T = −90 °C, Z = 2, $\rho_{calcd.}$ = 1.539 g cm^{-3}, μ(Mo-K_α) = 16.6 cm^{-1}, F(000) = 1464, 22044 reflections in h(−16/14), k(−19/18), l(−21/21), measured in the range 3.91° ≤ Θ ≤ 27.49°, completeness Θ_{max} = 98.5%, 14161 independent reflections, R_{int} = 0.031, 10601 reflections with $F_o > 4\sigma(F_o)$, 760 parameters, 12 restraints, $R1_{obs}$ = 0.067, wR^2_{obs} = 0.169, $R1_{all}$ = 0.096, wR^2_{all} = 0.192, GOOF = 1.032, largest difference peak and hole: 2.672/−1.039 e Å^{-3}.

Crystal data for L3. $C_{42}H_{26}N_4{\cdot}C_7H_7$, M_r = 677.79 g mol^{-1}, colourless prism, size 0.06 × 0.06 × 0.05 mm^3, triclinic, space group $P\bar{1}$, a = 11.3762(6), b = 12.7563(7), c = 13.6865(5) Å, α = 97.221(3), β = 102.933(3), γ = 110.078(2)°, V = 1773.1(1) Å^3, T = −90 °C, Z = 2, $\rho_{calcd.}$ = 1.270 g cm^{-3}, μ(Mo-K_α) = 0.75 cm^{-1}, F(000) = 710, 12620 reflections in h(−14/14), k(−15/16), l(−17/17), measured in the range 2.08° ≤ Θ ≤ 27.46°, completeness Θ_{max} = 98.8%, 8025 independent reflections, R_{int} = 0.033, 4464 reflections with $F_o > 4\sigma(F_o)$, 451 parameters, 0 restraints, $R1_{obs}$ = 0.089, wR^2_{obs} = 0.243, $R1_{all}$ = 0.152, wR^2_{all} = 0.293, GOOF = 1.027, largest difference peak and hole: 0.779/−0.488 e Å^{-3}.

CCDC reference numbers 290998 and 290999.

For crystallographic data in CIF or other electronic format see DOI: 10.1039/b512773d

Electronic spectroscopy

UV-vis absorption spectra (accuracy ±2 nm) were recorded on a Varian Cary 50 Scan spectrometer interfaced with a Dell optiplex GXI PC using Win UV Scan Application 2.00 and on an Analytikjena Specord S 600 spectrometer with standard software based tools. Emission spectra (accuracy ±5 nm) were recorded at 298 K using a Perkin-Elmer LS50B luminescence spectrophotometer, which was equipped with a red sensitive Hamamatsu R298 PMT detector and interfaced with an Elonex PC466 employing Perkin-Elmer Fl WinLab custom built software. Emission and excitation slit widths were 10 nm. Emission spectra for the ligands **L2** to **L4** were recorded at only 1% transmission due to large emission intensities. Emission spectra are uncorrected for photomultiplier response. 10 or 2 mm path length quartz cells were used for recording spectra.

Emission lifetime measurements

Luminescence lifetime measurements were obtained using an Edinburgh Analytical Instruments (EAI) time-correlated single-photon counting apparatus (TCSPC) comprised of two model J-yA monochromators (emission and excitation), a single photon photomultiplier detection system model 5300, and a F900 nanosecond flashlamp (N2 filled at 1.1 atm pressure, 40 kHz or 0.3 atm pressure, 20 kHz) interfaced with a personal computer *via* a Norland MCA card. A 410 nm cut off filter was used in emission to attenuate scatter of the excitation light (337 nm); luminescence was monitored at the λ_{max} of the emission. Data correlation and manipulation was carried out using EAI F900 software version 6.24. Samples were deaerated for 30 min using argon prior to measurements followed by repeated purging to ensure complete oxygen exclusion. Emission lifetimes were calculated using a single-exponential fitting function, Levenberg–Marquardt algorithm with iterative deconvolution (Edinburgh instruments F900 software). The reduced χ^2 and residual plots were used to judge the quality of the fits. Lifetimes are ±5%.

Resonance Raman spectroscopy

The Fourier transform off resonance FT-Raman spectrum of the solid complex **RuL1** was recorded with a Bruker IFS 120 HR spectrometer with an integrated FRA 160 Raman module and liquid nitrogen cooled germanium detector. The 1064 nm radiation of a Nd:YAG laser was employed for excitation. The non-resonant Raman spectra of the solid complex $[Ru(tbbpy)_3]^{2+}$ excited at 830 nm was taken with a micro Raman setup (LabRam invers, Jobin–Yvon–Horiba). The spectrometer has a focal length of 800 mm and is equipped with 300 lines/mm grating. The applied laser power was about 8 mW. The scattered light was detected by a CCD camera operating at 220 K. An Olympus MLPlanFL 50 objective focused the laser light on the solid samples.

The resonance Raman spectra were recorded with a conventional 90°-scattering arrangement. The excitation lines at 514.5, 488 and 458 nm provided by an argon ion laser (Spectra Physics Model 2085) served for resonant excitation in the range of the MLCT absorption band (see Fig. 7 later). To avoid the heating of the samples a rotating cell was utilized. No changes in the absorption spectra of the complexes could be observed after exposure to the resonant laser light. Moreover, the spectral lines observed under resonant conditions were also present in the off-resonant spectrum of the solid complexes, which was obtained with excitation at 830 nm. These findings indicate that the scattering due to possible photoproducts was minimal. The scattered light was collected with a photo objective (f = 50 mm, 1 : 0.7) and analysed with a Spex 1404 double monochromator. The dispersed Raman stray light was detected with a Photometrics model RDS 200 CCD Raman detector system. The concentration of the solutions was optimized to obtain a maximum signal-to-noise ratio and was in the millimolar range.

Results and discussion

Synthesis

All complexes under investigation are based on 4,4′-di-*tert*-butyl-2,2′-bipyridine (tbbpy) to increase the solubility of the ruthenium complexes in less polar organic solvents. This is helpful during the development of new synthetic methods which rely on organometallic reactions.[32,33] The new ligands **L1** to

L4 rely on the accessibility of 4,5-diamino-1,2-dibromobenzene which was conveniently prepared using literature methods[27] and coupled to phenanthrolin-5,6-dion resulting in 11,12-dibromo-dipyrido[3,2-*a*:2′,3′-*c*]-phenazine (**L1**) in nearly quantitative yield. Both bromine functions in **L1** are easily substituted by aromatics using conventional Suzuki-reactions utilising $\{Pd(P(Ph)_3]_4\}$ as catalyst yielding **L2**–**L4** in good yields (see Fig. 2).

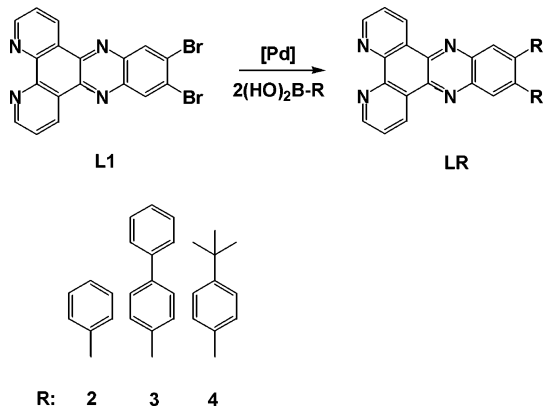

Fig. 2 Synthetic route to aryl substituted dppz ligands.

The nature of the products was unambiguously identified using multidimensional NMR methods, MS and UV-vis/emission spectroscopy. In addition the X-ray structure of **L3**, is shown in Fig. 3. The dppz frame is nearly ideally planar (deviation from planarity 0.038 Å) whereas the two biphenyl substituents are twisted out of the dppz plane by 47° (C16, C17, C19, C24) and 39° (C17, C16, C31, C36).

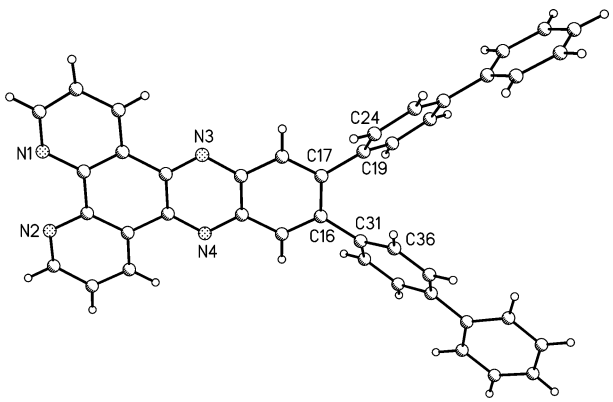

Fig. 3 Solid-state structure of **L3**.

Complexation of **L1**–**L4** to $(tbbpy)_2Ru^{2+}$ fragments [Ru] is achieved using microwave irradiation.[26] The full characterisation of all complexes with multidimensional NMR methods, MS and UV-vis/emission spectroscopy is outlined in the experimental part and in Table 1. In addition the solid-state structure of **RuL1** has been determined and is shown in Fig. 4. In the solid state structure of **RuL1** the deviation from planarity within the Br_2dppz ligand is 0.038 Å which is negligible. That there is a significant π–π interaction between neighbouring Br_2dppz moieties is apparent in the solid state with a distance of 3.54 Å between the centroid of the pyrazine ring and the plane of the C13–C18 aromatic ring in the ligand of the neighbouring complex at $(1 - x, 2 - y, 1 - z)$ as can be seen in Fig. 4. This arrangement is very similar to 11,12-dicyano-dppz ruthenium complexes.[34]

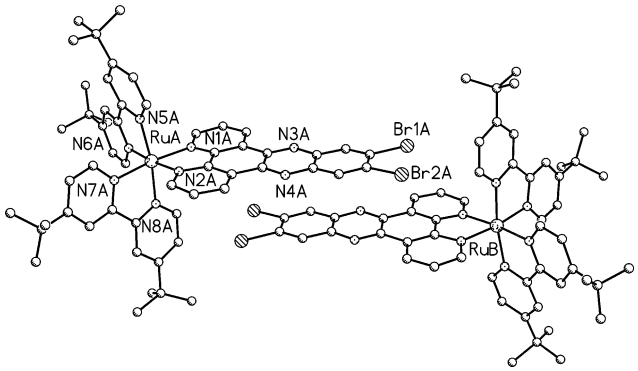

Fig. 4 Solid-state structure of **RuL1** relevant bond length in Å: Ru–N1 2.063(4), Ru–N2 2.065(4), Ru–N5 2.051(4), Ru–N6 2.052(4), Ru–N7 2.053(4), Ru–N8 2.056(4), Br1–C15 1.880(5), Br2–C16 1.894(5); and angles in °: N1–Ru–N2 79.16(16), N5–Ru–N6 78.61(16), N7–Ru–N8 78.17(17); additional "A" letter indicates symmetry equivalent position of the complex at $(1 - x, 2 - y, 1 - z)$.

The successful transformation of the cationic ruthenium complex **RuL1** using the Suzuki-protocol into **RuL2**, with 70% yield, illustrates the potential of organometallic coupling reactions (see Fig. 5) to selectively modify precursor complexes.[32,33] No significant advantages were identified when comparing the organometallic coupling reactions starting from **L1** or **RuL1**. Suzuki coupling of the complexed ligand opens however the route towards the introduction of substituents representing potential coordination sites, such as different pyridines, which would interfere with complexation if introduced into the free ligand.

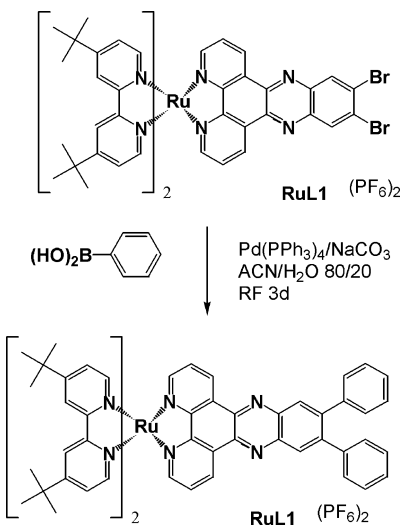

Fig. 5 Complex based Suzuki-reactions.

Electronic properties

All four ligands display absorption maxima around 400 nm. A clear influence of the peripheral substitution pattern on the shape

Table 1 Photophysical properties of **L1**–**L4** and **RuL1** to **RuL4**[a]

Complex	Emission-DCM	Emission-ACN	Absorption in DCM $\lambda_{max,abs}$/nm	Absorption in ACN $\lambda_{max,abs}$/nm	τ-DCM-aerated/ns	τ-DCM-deaerated/ns	τ-ACN-aerated/ns	τ-ACN-deaerated/ns
L1(Br_2)	420	—	237 (sh 297), 373, 392	—	[b]	—	—	—
L2(Ph)	433	—	(sh 374), 394	—	0.59	—	—	—
L3(BPh)	470	—	233, 297, 408	—	2.22	—	—	—
L4(TBPh)	455	—	229, 286, 406	—	1.65	—	—	—
RuL1	645	—	287, 374, 390, 444	287, 370, 386, 442	258	453	—	—
RuL2	631	654	290 (sh 320), 405 (sh 450)	288 (sh 317), 399 (sh 440)	406	779	129	201
RuL3	630	654	291, 424 (sh 480)	288, 414 (sh 480)	452	807	118	180
RuL4	625	650	290 (sh 338), 418 (sh 475)	288 (sh 328), 411 (sh 468)	502	929	129	245

[a] ACN acetonitrile, DCM dichloromethane. [b] Emission intensity was too weak to obtain an accurate lifetime using our set-up.

of the long wavelength maxima is observed. For example, **L1** features two distinct maxima at 393 nm and 374 nm (shoulder at 381 nm). similar to unsubstituted dppz.[13] The introduction of aromatic substituents leads to a red shift of the absorption maxima and loss of the band at around 370 nm. The bathochromic shift is most pronounced for the bi-biphenyl substituted **L3**. This ligand shows only a single broad absorption at 408 nm. All three aromatically substituted ligands (**L2** to **L4**) show relatively strong emission signals between 433 (**L2**) nm and 470 (**L3**) nm in dichloromethane, see Fig. 6, whereas **L1** displays only very weak emission at 420 nm. The largest stokes shift (>60 nm) is observed for the biphenyl substituted **L3**.

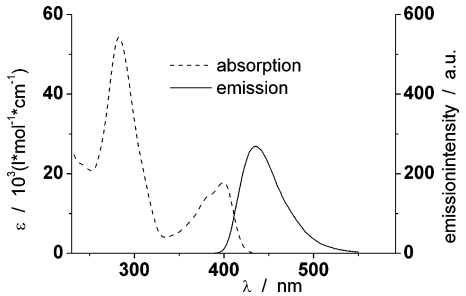

Fig. 6 Absorption and emission spectra of **L2** in dichloromethane solution (c(**L2**) = 8.6 × 10^{-6} mol l^{-1}).

The excited state lifetimes of **L2**–**L4** have been determined. They range from 0.6 to 2 ns, (see Table 1). The absorption and emission data of **L1** to **L4** indicate that the substitution of the dppz frame with aromatic moieties results in very significant changes in the electronic properties of the ligands. It is important at this stage to note that since the ligand based electronic transitions of the LR ligands are at least partly in the visible range of the spectrum and therefore in the same range as those expected for ruthenium polypyridyl-type MLCT the lowest energy transition in a corresponding complex may contain significant π–π* character.

All four complexes show absorption properties which are common for this class of ruthenium polypyridyl compounds. Their oxidation potential is not affected by the peripheral substitution at the dppz ligand and is observed at 0.82 V *vs* Fc/Fc^+. This suggests that the introduction of the substituents has no significant influence on the metal based ground state. The absorption spectra in acetonitrile are depicted in Fig. 7. The absorption spectrum of **RuL1** is very similar to the related compound $[Ru(bpy)_2dppz]^{2+}$ showing a MLCT band at 444 nm and a dppz based π–π* transition at shortly below 400 nm.[15] Introduction of more extensive aromatic substituents leads to a red shift of the π–π* transition, which ultimately overlaps increasingly with the Ru-π* MLCT band. This results in an increase of the extinction within the MLCT region from 17 000 for **RuL1** at 444 nm to 26 000 for **RuL3** at 414 nm.

The luminescence data for all four complexes could be obtained in acetonitrile and dichloromethane. A profound influence of the solvent on emission wavelength is evident by the *ca.* 20 nm red shift of the emission wavelength upon going from dichloromethane to acetonitrile. Similar solvent dependencies have been reported for related ruthenium–dppz complexes.[37,38] The most obvious impact of substitution at the dppz core is observed for **RuL1**, which is non-emissive even in CaH_2 dried acetonitrile, whereas relatively

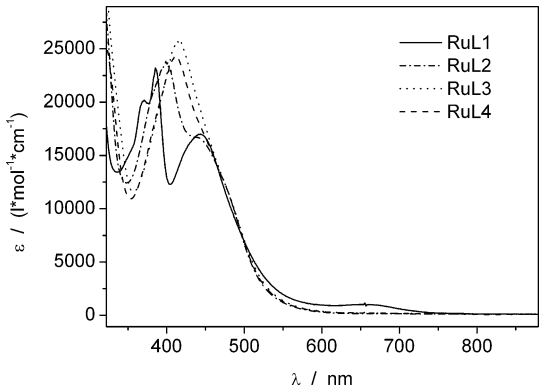

Fig. 7 Absorption spectra of **RuL1** to **RuL4** in acetonitrile.

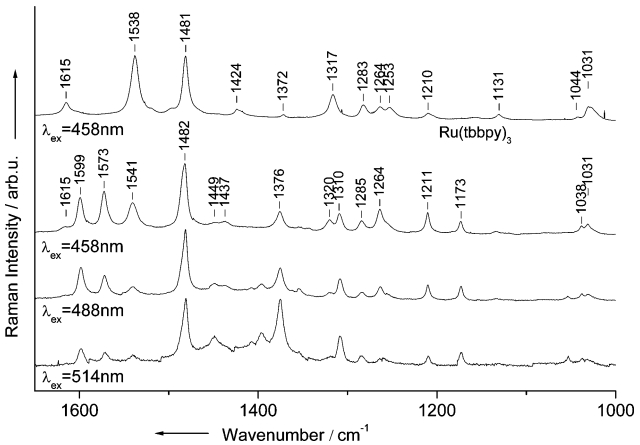

Fig. 8 Resonance Raman spectra of **RuL1** dissolved in acetonitrile excited at three different wavelength (514, 488, 458 nm) lying within the first absorption band of **RuL1**(see Fig. 7). The resonance Raman band of $[Ru(tbbpy)_3]^{2+}$ dissolved in dichloromethane excited at 458 nm in resonance close to the maximum of the first absorption and is shown for comparison. For details see text.

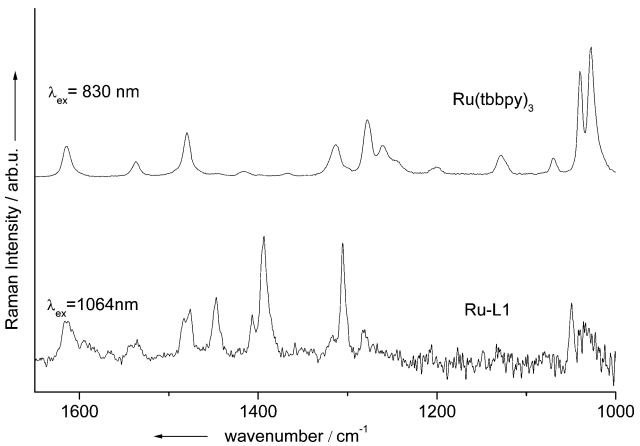

Fig. 9 Off resonance Raman spectra of **RuL1**(λ_{exc} = 1064 nm) and $[Ru(tbbpy)_3]^{2+}$ (λ_{exc} = 830 nm).

strong luminescence is observed in dichloromethane. A trend of prolonged lifetimes for the aryl substituted complexes **RuL2**–**RuL4** is evident with the longest lifetime of 929 ns observed for **RuL4** in dichloromethane. The investigation of the lifetimes of the excited state of all complexes in both solvents reveals also a strong solvent dependency. All lifetimes in acetonitrile are only about 25% of the values obtained in dichloromethane. The lifetime of the excited states of **RuL1** in dichloromethane is comparable with literature values obtained for the monobromo-dppz ruthenium complex.[15] Detailed photophysical data are compiled in Table 1.

Resonance Raman of RuL1

Resonance Raman spectroscopy is an extremely capable tool to characterise the molecular degrees of freedom involved in the initial structural changes of photochemically active systems *i.e.* to characterise the Franck–Condon-Point of an electronic transition. The resonance condition arises when the wavelength used to excite the Raman scattering lies within the electronic absorption band, causing the vibrational modes involved in the electronic transition to be selectively enhanced (by a factor of 10^6 compared to non-resonant excitation). Resonance Raman spectroscopy is therefore the method of choice for investigating the location of the initially formed MLCT in heteroleptic complexes where two different ligand sites are possible.

Fig. 8 shows the resonance Raman spectra of **RuL1** excited at three different wavelengths within the first MLCT transition. The vibrational modes at 1599, 1573, 1330 and 1173 cm^{-1} grow in intensity when the excitation wavelength is shifted from 514 nm at the red edge of the absorption band to 458 nm near the maximum of the lowest energy absorption feature and these modes can be assigned to the **L1**-ligand. This is confirmed by the comparison between the resonance Raman spectrum of **RuL1** with that of $[Ru(tbbpy)_3]^{2+}$. The main modes enhanced in the resonance Raman spectrum of **RuL1** are not observed in the spectrum of the latter compound and must therefore be due to **L1**. This assignment is further supported by looking at the off resonance Raman spectra of both molecules plotted in Fig. 9. The fact that the modes which are enhanced most belong to the **L1**-ligand leads us to the conclusion that exciting **RuL1** within the MLCT transition at 458 nm involves mainly the **L1**-ligand rather than tbppy.

Importantly, however, other modes seen in the resonance Raman spectrum at 1615, 1541, 1376, 1320 and 1211 cm^{-1} might be due to tbbpy. The fact that possibly also tbbpy-modes may be enhanced suggests that Ru-to-tbbpy-type MLCT transitions may also contribute to the absorption envelop. This assignment is based on literature values from Meyer *et al.*[39] and McGarvey *et al.*[20] Theoretical calculations which are currently under way may help to shed more light on this issue.[40]

Conclusion

In conclusion we have shown that it is possible to obtain ruthenium polypyridyl-type complexes containing substituted dppz-type ligands using Suzuki coupling reactions starting either from the free ligand dibromo-dppz, **L1**, or from its ruthenium complex **RuL1**. For the compounds reported in this contribution the results obtained from both synthetic approaches are very similar. However, the use of a metal complex rather than the free ligand offers significant advances when the substituents to be introduced either have coordinating properties or would not be stable at

the high temperature conditions needed to prepare the metal compounds.

The second important observation is that the absorption spectra of the free ligands are very dependent on the substitution pattern. Importantly, with increasing aryl character the ligand centred π–π* transition of the LR ligand moves to lower energy and overlaps considerably with the MLCT transition. This effect has two potentially important consequences; one relates to the application of the ruthenium dppz complexes as luminescent sensors, in that higher extinction coefficients in the visible region will result in a better sensor (ruthenium complex) to analyte (for instance DNA) ratio.

In addition this shift may affect the so called "dark state" of the dppz molecule.[35] The importance of intraligand electron transfer, from the initially populated bpy ^{1}MLCT to the phenazine based ^{3}MLCT for explaining the unusual light switch mechanism observed for the ruthenium dppz complexes has recently been emphasised by Batista and Martin.[36] Expansion of the aromatic frame as evident in **L2** to **L4** may be expected to influence the rate constants for this process and therefore lead to new insights into this phenomenon.

Acknowledgements

Financial support by the DFG (SFB 436) is gratefully acknowledged. S.R. acknowledges financial support by the DFG (RA 1017/1-1 and 1-2). W.H. would like to thank Enterprise Ireland (Grant Number SC/2003/74) for financial support. We would like to thank Professor D. Walther for helpful discussions and encouragement.

References

1 J. K. Barton, A. T. Danishefsky and J. M. Goldberg, *J. Am. Chem. Soc.*, 1984, **106**, 2172.
2 J. M. Kelly, A. B. Tossi, D. J. McConnell and C. OhUigin, *Nucleic Acids Res.*, 1985, **13**, 6017.
3 J. K. Barton, J. M. Goldberg, C. V. Kumar and N. J. Turro, *J. Am. Chem. Soc.*, 1986, **108**, 2018.
4 C. Hiort, B. Nordén and A. Rodger, *J. Am. Chem. Soc.*, 1990, **112**, 1971.
5 A. E. Friedman, J. C. Chambron, J.-P. Sauvage, N. J. Turro and J. K. Barton, *J. Am. Chem. Soc.*, 1990, **112**, 4960.
6 B. Lincoln, A. Broo and B. Nordén, *J. Am. Chem. Soc.*, 1996, **118**, 2644.
7 C. G. Coates, L. Jacquet, J. J. McGarvey, S. E. J. Bell, A. H. R. Al-Obaidi and J. M. Kelly, *J. Am. Chem. Soc.*, 1997, **119**, 7130.
8 I. D. Greguric, J. R. Aldrich-Wright and J. G. Collins, *J. Am. Chem. Soc.*, 1997, **119**, 3621.
9 Y. Jenkins, A. E. Friedman, N. J. Turro and J. K. Barton, *Biochemistry*, 1992, **31**, 10809.
10 C. G. Coates, J. Olofsson, M. Coletti, J. J. McGarvey, B. Önfelt, B. Lincoln, B. Nordén, E. Tuite, P. Matousek and A. W. Parker, *J. Phys. Chem. B*, 2001, **105**, 12653.
11 G. Pourtois, D. Beljonne, C. Moucheron, S. Schumm, A. Kirsch-De Mesmaeker, R. Lazzaroni and J.-L. Bredas, *J. Am. Chem. Soc.*, 2004, **126**, 683.
12 D. A. McGovern, A. Selmi, J. E. O'Brien, J. M. Kelly and C. Long, *Chem. Commun.*, 2005, 1402.
13 W. Chen, C. Turro, L. A. Friedman, J. K. Barton and N. J. Turro, *J. Phys. Chem. B*, 1997, **101**, 6995.
14 P. Aguirre, R. López, D. Villagra, I. Azocar-Guzman, A. J. Pardey and S. A. Moya, *Appl. Organomet. Chem.*, 2003, **17**, 36.
15 N. J. Lundin, P. J. Walsh, S. L. Howell, J. J. McGarvey, A. G. Blackman and K. C. Gordon, *Inorg. Chem.*, 2005, **44**, 3551 and references cited therein.
16 M. K. Kuimova, W. Z. Alsindi, J. Dyer, D. C. Grills, O. S. Jina, P. Matousek, A. W. Parker, P. Portius, X. Zhong Sun, M. Towrie, C. Wilson, J. Yang and M. W. George, *Dalton Trans.*, 2003, 3996.
17 P. Y. Chen and T. J. Meyer, *Chem. Rev.*, 1998, **98**, 1439.
18 E. Amouyal, A. Homsi, J.-C. Chambron and J.-P. Sauvage, *J. Chem. Soc., Dalton Trans.*, 1990, (6), 1841.
19 E. M. Kober and T. J. Meyer, *Inorg. Chem.*, 1982, **21**, 3967.
20 C. G. Coates, P. Callaghan, J. J. McGarvey, J. M. Kelley, P. E. Kruger and M. E. Higgins, *J. Raman Spectrosc.*, 2000, **31**, 283.
21 J.-C. Chambron and J.-P. Sauvage, *Chem. Phys. Lett.*, 1991, **182**, 603.
22 J. Olofsson, B. Önfelt, B. Lincoln, B. Nordén, P. Matousek, A. W. Parker and E. Tuite, *J. Inorg. Biochem.*, 2002, **91**, 286.
23 V. W.-W. Yam, V. W.-M. Lee, F. Ke and K.-W. M. Siu, *Inorg. Chem.*, 1997, **36**, 2124.
24 J. K. Barton, L. A. Basile, A. Danishefsky and A. Alexandrescu, *Proc. Natl. Acad. Sci. U. S. A.*, 1984, **81**, 1961.
25 P. P. Pellegrini and J. R. Aldrich-Wright, *Dalton Trans.*, 2003, 176.
26 S. Rau, B. Schäfer, A. Grüßing, S. Schebesta, K. Lamm, J. Vieth, H. Görls, D. Walther, M. Rudolph, U. W. Grummt and E. Birkner, *Inorg. Chim. Acta*, 2004, **357**, 4496.
27 G. W. H. Cheeseman, *J. Chem. Soc. C*, 1962, 1170.
28 *COLLECT, Data Collection Software*, Nonius B.V., Netherlands, 1998.
29 Z. Otwinowski and W. Minor, Processing of X-Ray Diffraction Data Collected in Oscillation Mode, in *Methods in Enzymology, vol. 276. Macromolecular Crystallography, Part A*, ed. C. W. Carter and R. M. Sweet, Academic Press, 1997, pp. 307–326.
30 G. M. Sheldrick, *Acta Crystallogr. Sect. A*, 1990, **46**, 467.
31 G. M. Sheldrick, *SHELXL-97 (Release 97-2)*, University of Göttingen, Germany, 1997.
32 R. Passalacqua, F. Loiseau, S. Campagna, Y.-Q. Fang and G. S. Hanan, *Angew. Chem., Int. Ed.*, 2003, **42**, 1608.
33 C. J. Aspley and J. A. Gareth Williams, *New J. Chem.*, 2001, **25**, 1136.
34 J. Rusanova, S. Decurtins, E. Rusanov, H. Stoeckli-Evans, S. Delahaye and A. Hauser, *Dalton Trans.*, 2002, 4318.
35 Matthew K. Brennaman, T. J. Meyer and J. M. Papanikolas, *J. Phys. Chem. A*, 2004, **108**, 9938.
36 E. R. Batista and R. L. Martin, *J. Phys. Chem. A*, 2005, **109**, 3128.
37 K. O'Donoghue, J. C. Penedo, J. M. Kelly and P. E. Kruger, *Dalton Trans.*, 2005, 1123.
38 R. S. Nair, B. M. Cullum and C. J. Murphy, *Inorg. Chem.*, 1997, **36**, 962.
39 J. R. Schoonover, W. D. Bates and T. J. Meyer, *Inorg. Chem.*, 1995, **34**, 6421.
40 See for instance S. Fantacci, F. DeAngelis, A. Sgamellotti and N. Re, *Chem. Phys. Lett.*, 2004, **396**, 43–48.